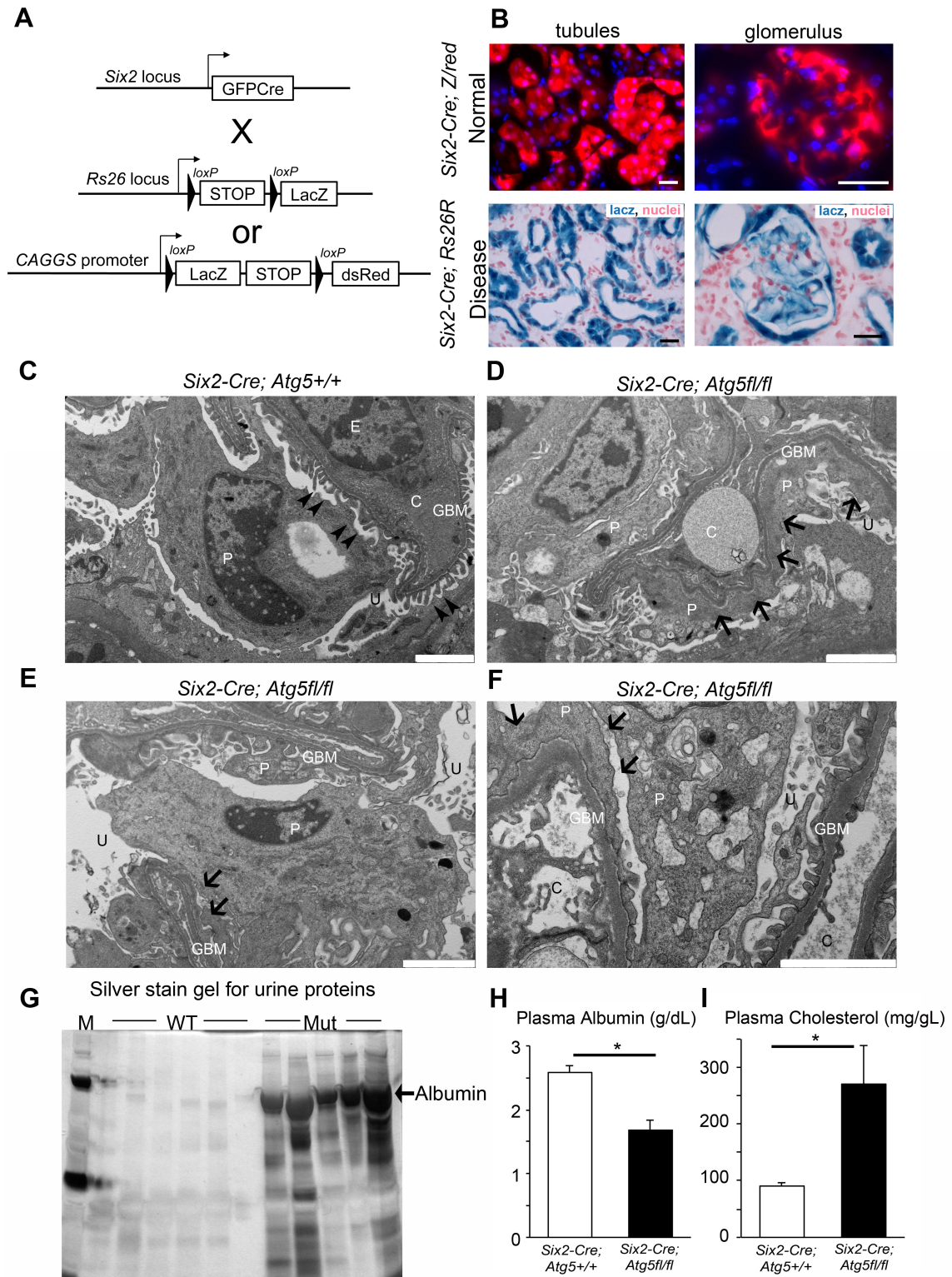
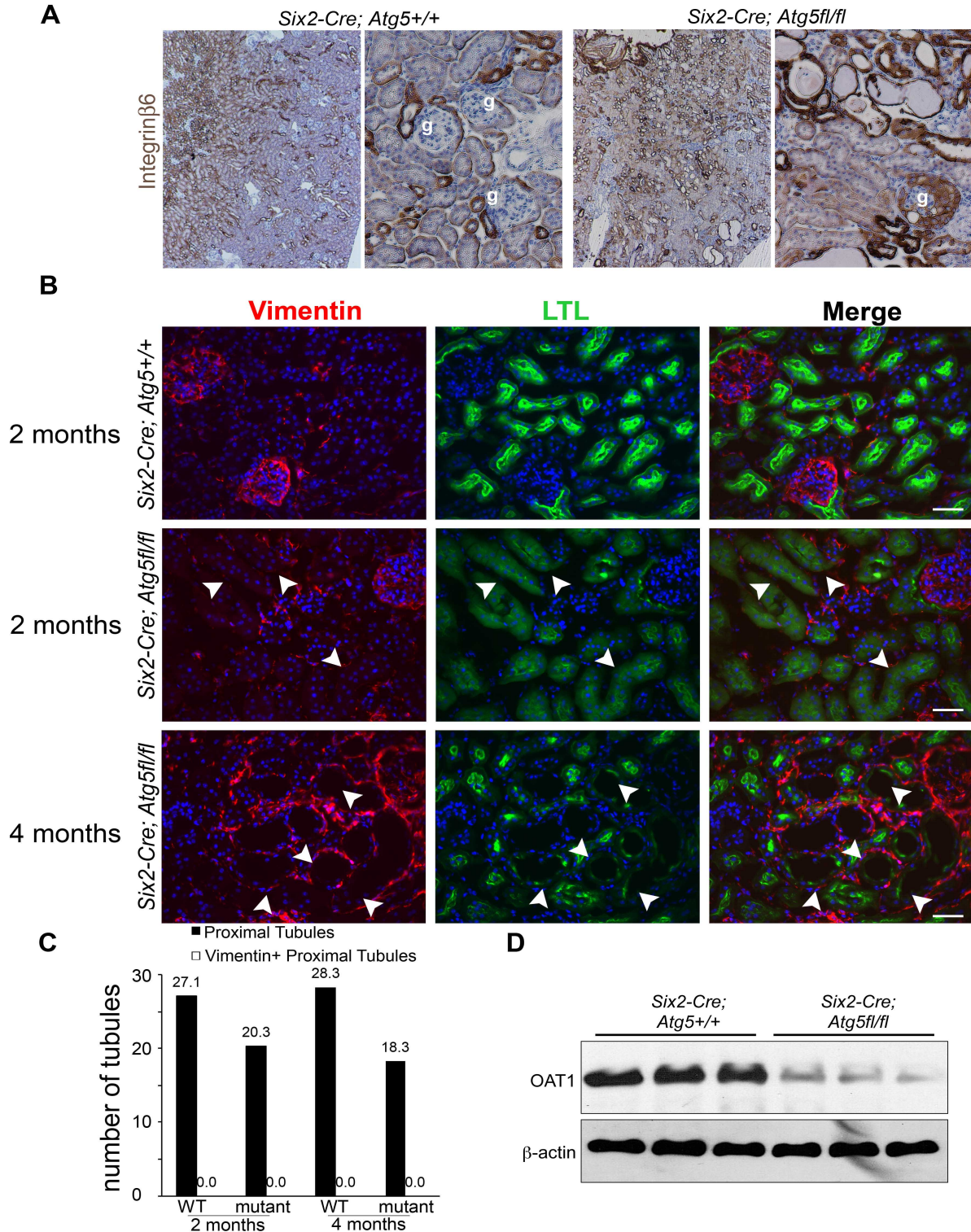


**SUPPLEMENTAL INFORMATION**

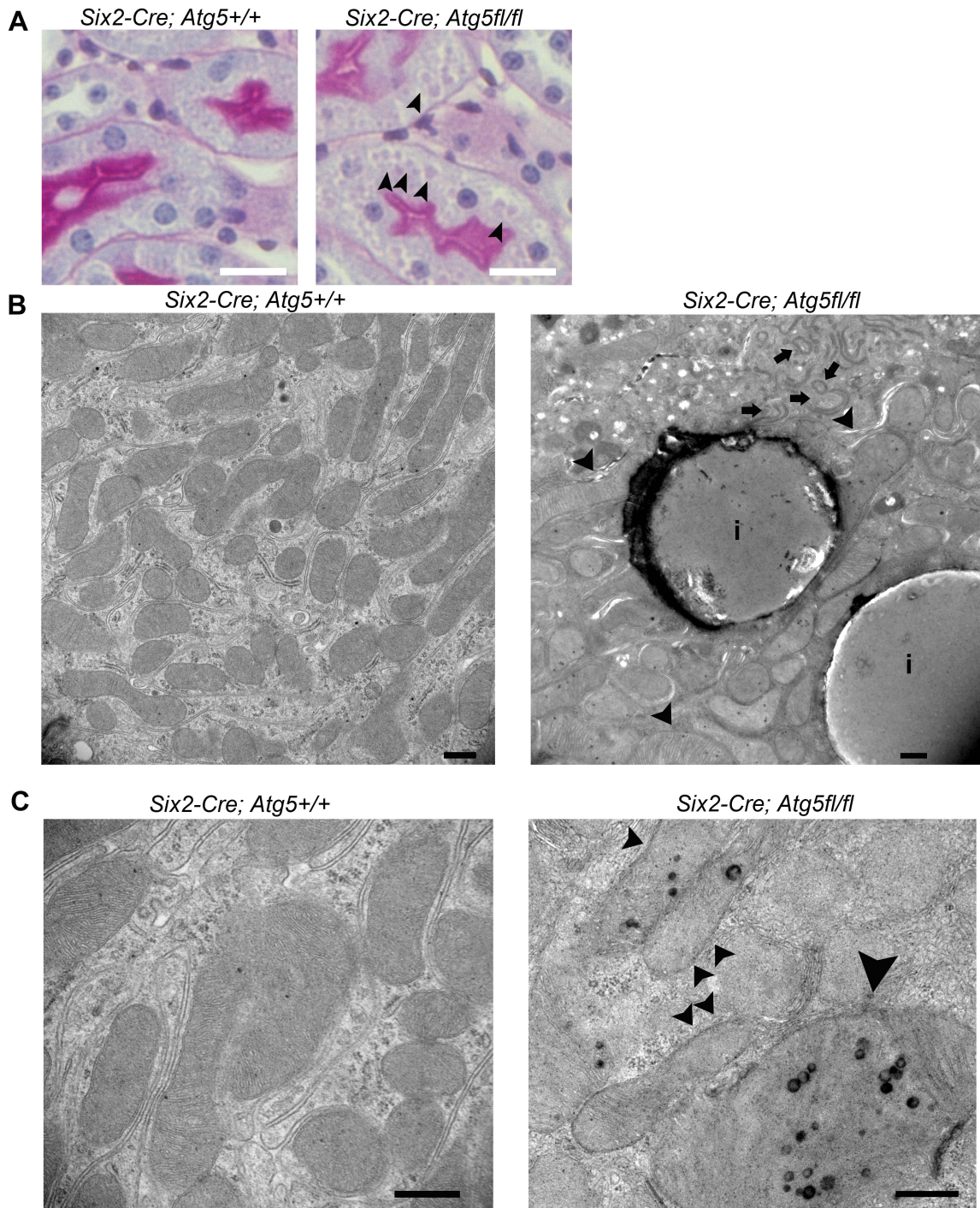


**Supplemental Figure 1. Characterization of recombination of epithelial progenitors by Six2-Cre and characterization of disease at 4 months in Six2-Cre; Atg5<sup>fl/fl</sup> mice.** (A-B) Schema and images showing Six2-Cre BAC transgene catalyzes highly efficient recombination at *loxP* sites in epithelial progenitors during nephrogenesis, resulting in widespread activation of fluorescent or enzymatic reporters in all epithelial cells of the glomerulus, and nephron. Images from Six2-Cre; Z/Red kidneys and Six2-Cre; Rs26R kidneys showing efficient recombination in podocytes and tubules (except collecting duct) where recombination occurs in >98% of all non-collecting duct epithelial cells. (C-F) EM images showing widespread foot process effacement at 4 months in mutant glomeruli but not WT glomeruli (U = urinary space, GBM = glomerular basement membrane, P = podocyte, C = capillary loop, arrowheads = foot processes, arrows show foot process effacement. Bar = 2µm) (G) Silver stained SDS-PAGE gradient gel showing proteins in urine of mutant mice at 4 months compared to WT (M = molecular size marker). Note albumin (69kDa) is the dominant protein (H-I) Plasma levels of Albumin and cholesterol in mice at 4 months (n= 5-6/group, \*  $P < 0.05$ , \*\*  $P < 0.01$ )



**Supplemental Figure 2. Tubule cells do not acquire vimentin expression in *Six2-Cre; Atg5<sup>fl/fl</sup>* mice but they upregulate integrin- $\beta$ 6 and lose the organic anion transporter OAT-1**

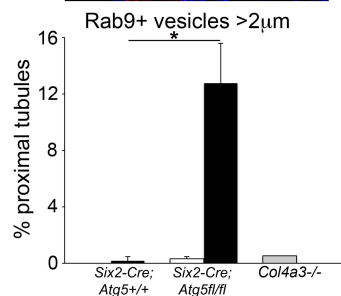
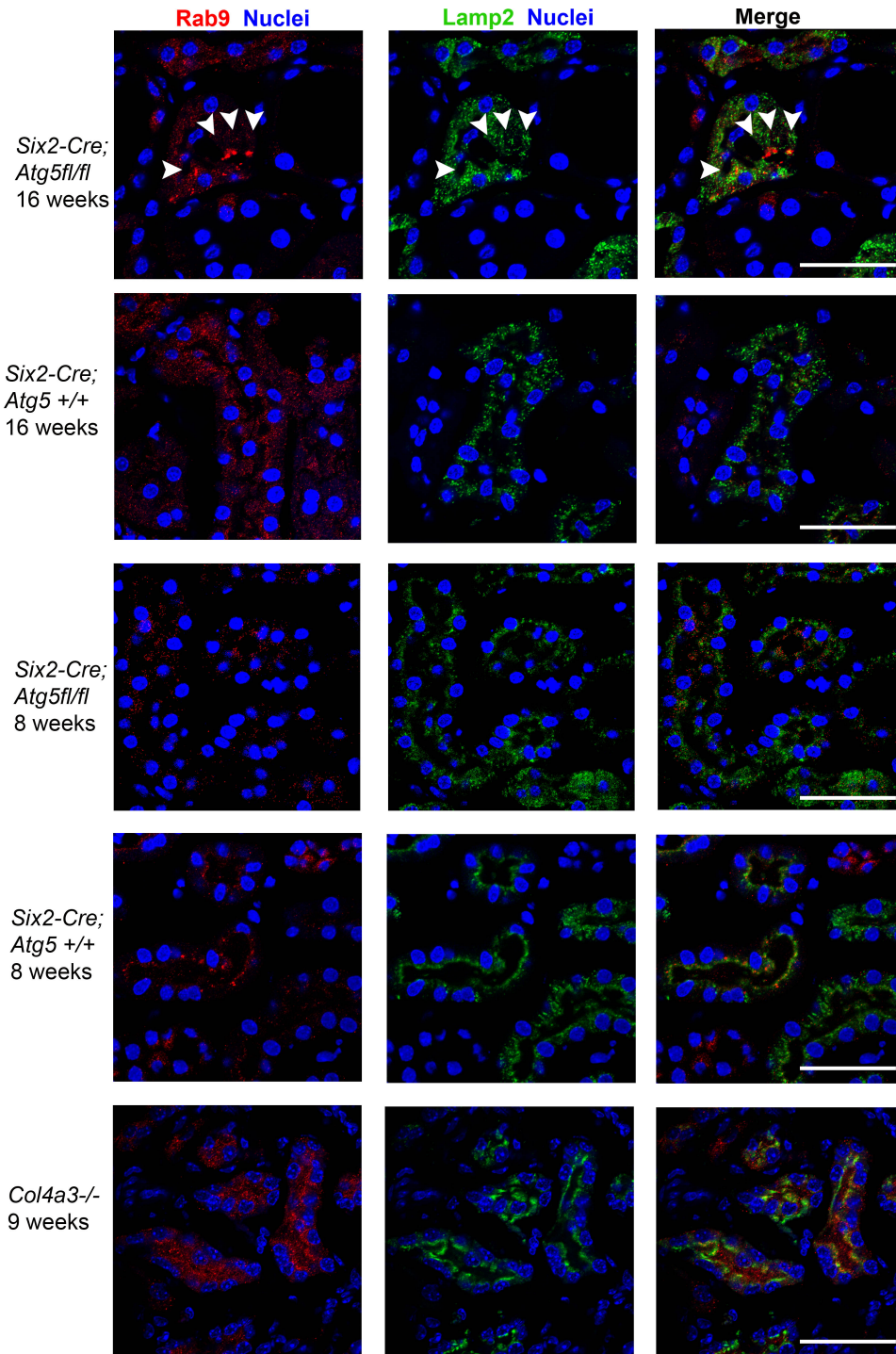
(A) Expression of integrin- $\beta$ 6 in tubule cells at 4 months. Note proximal and distal tubule cells in the cortex and glomerulus express  $\beta$ 6 minimally at the basolateral surface but in disease GECs and proximal and distal tubule cells markedly upregulate cortical expression (Bar = 50 $\mu$ m). (B-C) Split panel photomicrographs showing and graph quantifying expression of the mesenchymal marker vimentin in healthy and mutant kidneys at 2 months and 4 months. Note that although there is expression of vimentin in normal kidney and expansion of vimentin+ interstitial cells that none of the LTL co-stained epithelium co expresses vimentin. Arrowheads show injured epithelium which does not co-express vimentin (bar = 50 $\mu$ m). (D) Western blot of whole kidney showing expression of the proximal tubule basolateral transporter OAT-1, critical for tubule secretion at 2 months of age.



**Supplemental Figure 3. Tubule cells have inclusion bodies and mitochondrial abnormalities in 2 month old mutant kidneys.**

(A) PAS stained proximal tubules from 2 month old kidneys showing intracellular inclusions localized to the basolateral side of cells (arrowheads) (bar = 50µm). (B-C) EM images showing tubular mitochondria, ER and inclusion bodies (i) at 2 months. Note

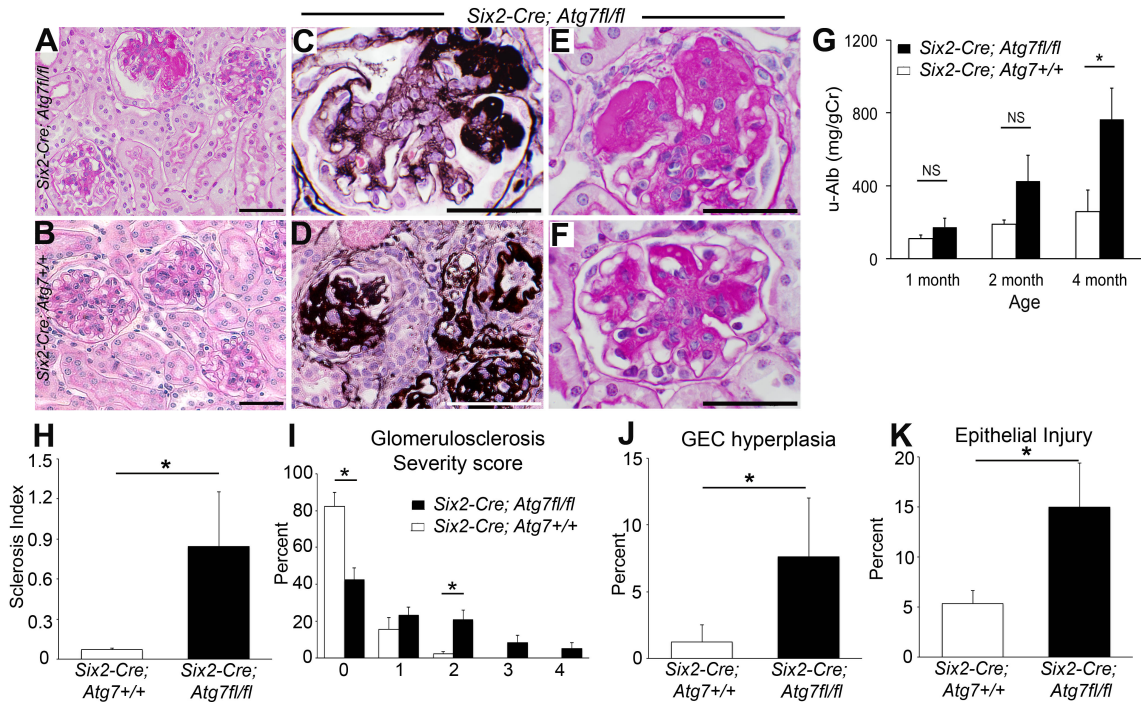
mutant mitochondria who increased size, with loss of elongation, and areas where there are no cristae (arrowheads). Also note very prominent and enlarged ER (small arrows). (bar = 500nm)



**Supplemental Figure 4.**

**Large Rab9+ LAMP2- vesicles occur specifically in Six2-Cre; Atg5fl/fl proximal tubules.**

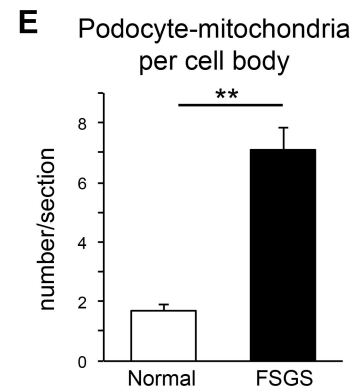
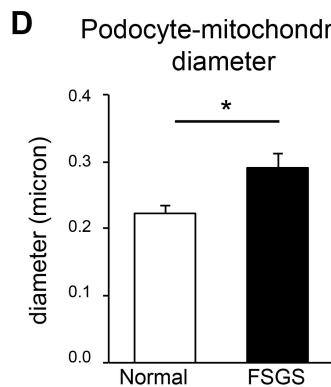
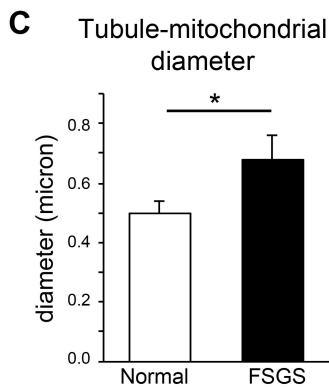
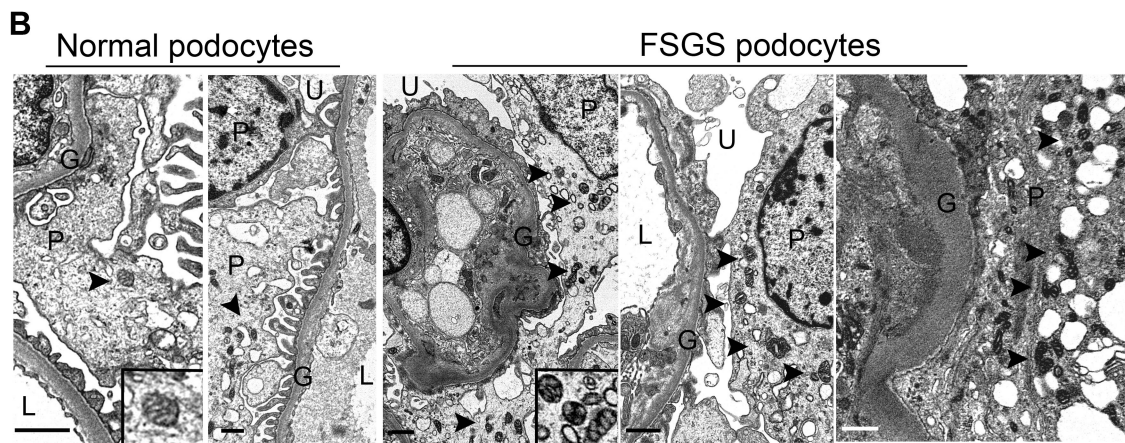
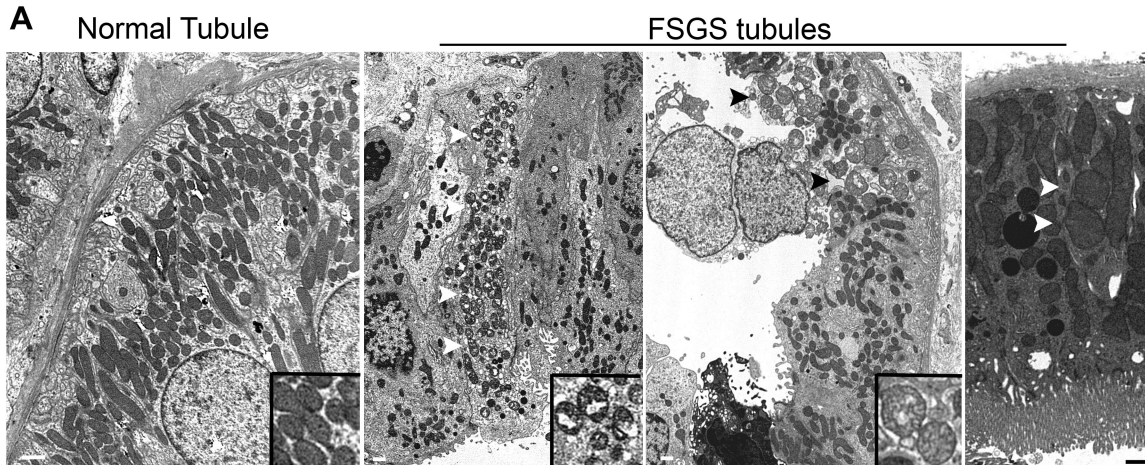
**(A)** Representative confocal images of LAMP2+ proximal tubules showing the presence of large intracellular compartments containing Rab9 but not co-localizing with LAMP2 (Quantification of large Rab9 vesicles (>2 $\mu$ m) in proximal tubules of mice. Note *Col4a3*<sup>-/-</sup> ‘Alport’ mice with severe kidney failure and tubule disease do not show similar vesicles in proximal tubules. **(B)** Graph showing number of tubule cross sections with Rab9 large vesicles. Data are means  $\pm$  SEM. \*  $P < 0.05$ .



**Supplemental Figure 5.**

**Mutation of ATG7 in kidney epithelial causes FSGS.**

**(A-B)** Representative images of glomerular changes between mutant and control **(C-F)** Typical glomerular morphology at 4 months after birth, stained by PAS or silver methenamine. Note the presence of segmental sclerotic lesions (fibrosis and capillary loop destruction) and focal glomerular involvement. **(G)** Graph showing urine Alb/Cr ratio in mice with time after birth. **(H-I)** Quantification of glomerulosclerosis by index or by % of glomeruli with sclerosis or severity score. **(J)** Quantification of glomeruli with GEC hyperplasia. **(K)** Quantification of tubular injury. Data are mean  $\pm$  SEM. n= 6/group. \*  $P < 0.05$ .



**Supplemental Figure 6.**

**Human idiopathic FSGS biopsies show tubular and podocyte mitochondrial abnormalities compared to healthy kidneys.**

(A) EM images showing healthy and diseased (FSGS) tubule mitochondria. Arrowheads highlight abnormal mitochondria and examples are shown in insets. Note mitochondrial enlargement, loss of elongation, and destruction of cristae. (B) EM images showing podocyte cell bodies in which increased mitochondrial numbers and size can be seen

(arrowheads) (C-F) Morphometry of tubular or podocyte mitochondria indicates increased mitochondrial diameter in both cell types and increased numbers of mitochondria in podocytes in FSGS patients (n= 10/group, \**P* < 0.05, \*\**P* < 0.01) (bar = 1µm)

## Supplemental Tables

### Supplemental Table 1

Plasma levels at 4 months showing mean +/- standard error (n= 6/group)

	Albumin g/dL	Cholesterol mg/dL	HDL mg/dL	Triglycerides mg/dL	LDL mg/dL	Free Fatty Acids mEq/L	BUN mg/dL
WILD TYPE	2.58 +/- 0.1	90.7 +/- 4.8	58 +/- 2.9	109 +/- 7.7	7.5 +/- 0.4	1.56 +/- 0.09	23.8 +/- 3.1
MUTANT	1.68 +/- 0.15	270.6 +/- 67.8	120.2 +/- 22.4	150.2 +/- 47.2	21.8 +/- 4.9	2.05 +/- 0.35	49.6 +/- 14.7